Kolbe-Schmitt reaction of sodium 2-naphthoxide

Zoran Marković[1], Svetlana Marković[2], Igor Đurović[2]

[1] Faculty of Agronomy, University of Kragujevac, Čačak, Serbia
[2] Faculty of Science, University of Kragujevac, Kragujevac, Serbia

Abstract The mechanism of the *Kolbe-Schmitt* reaction of sodium 2-naphthoxide is examined by means of the *B3LYP*/LANL2DZ method. After the initial formation of sodium 2-naphthoxide-CO_2 complex, the carbon of the CO_2 moiety performs an electrophilic attack on the naphthalene ring. Further transformations lead to the formation of sodium 2-hydroxy-1-naphthoate. Sodium 3-hydroxy-2-naphthoate is formed by a 1,3-rearrangement of the CO_2Na group. Our findings are in good agreement with the experimental results on the carboxylation reaction of sodium 2-naphthoxide.

Keywords *Kolbe-Schmitt* reaction; Sodium 2-naphthoxide; Reaction mechanism; *Ab initio* calculations; *B3LYP*/LANL2DZ.

Introduction

The *Kolbe-Schmitt* reaction is a carboxylation reaction of alkali and alkaline earth metal phenoxides or naphthoxides, where aromatic hydroxy acids are formed. The products of the *Kolbe-Schmitt* reaction play a significant role in the synthesis of numerous products, such as pharmaceuticals, antiseptic, fungicidal and color-developing agents, textile assistants, polyesters, high-polymeric liquid crystals, and dyes.

The carboxylation reaction of alkali metal phenoxides has been a subject of numerous experimental and theoretical investigations [1–14]. The mechanism of the *Kolbe-Schmitt* reaction of alkali metal phenoxides has been established by means of DFT methods [9–13], and the structure of the intermediate alkali metal phenoxide – carbon dioxide complex has been elucidated [14]. It has been shown that the yield of the *para* substituted product increased with increasing ionic radius of the alkali metal used [10, 13]. A quantitative explanation for this occurrence and the equilibrium behavior of the *Kolbe-Schmitt* reaction has been provided [9, 10]. The influence of solvent effects on the kinetics of the carboxylation reaction of sodium phenoxide has also been investigated [11, 12].

Sodium 2-naphthoxide (**1**) is another interesting reactand in the *Kolbe-Schmitt* reaction, because the reactivities at the positions 1, 3, and 6 are competitive with one another. A general outline of the carboxylation reaction of **1** is presented in Fig. 1.

Early investigations of the carboxylation reaction of **1** showed that a product, which has been considered to be ''sodium β-naphthyl carbonate'', has been formed at lower temperatures (40–60°C) [15]. The carbonate dissociated at higher temperatures into its components. Under the enhanced pressure of CO_2 and the temperature of 120°C the carbonate rearranged to 1-carboxy-2-sodium naphthoxide, whose structure has been proposed without experimental details. The intermediate carbonate has been considered to decompose to give ''active CO_2'', which then carbonated **1**. A similar reaction mechanism has

Correspondence: Svetlana Marković, Faculty of Science, University of Kragujevac, 34000 Kragujevac, Serbia, E-mail: mark@kg.ac.yu
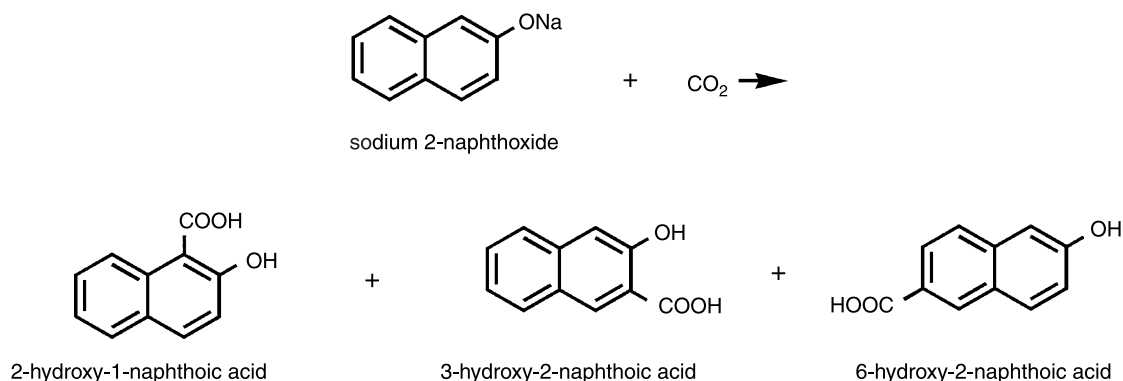
Fig. 1 Carboxylation reaction of sodium 2-naphthoxide (**1**)

been suggested by *Gershzon* [16], who prepared salicylanilide by treating the phenyl ester of phenylcarbamic acid with sodium in boiling xylene, and heating the intermediate $C_6H_5OC(=NC_6H_5)ONa$ in a sealed tube at 200°C. Under a similar treatment, the 1-naphthyl and 2-naphthyl esters yielded the corresponding hydroxynaphthoic anilides. It has been claimed that these experiments proved the intermediate formation of metal aryl carbonates in the *Kolbe-Schmitt* reaction. This consideration has been disproved by *Chelintsev* [17], who found that the products arising by treatment of the phenyl ester of phenylcarbamic acid with sodium have been diphenylurea and triphenyl isocyanurate. The triphenyl isocyanurate suggested the presence of phenyl isocyanate in the reaction mixture. It has been shown that salicylanilide has been formed by heating phenyl isocyanate with sodium phenoxide. *Hales* has considered that the initial reaction of CO_2 with metal aryloxide involved weak chelation of the gas with the metal to produce an unstable complex [4].

In a novel study, carboxylations of various alkali and alkaline earth metal 2-naphthoxides have been examined [7]. It has been shown that **1** needed to be heated above 200°C to produce a mixture of 2-hydroxy-1-naphthoic acid and 3- and 6-hydroxy-2-naphthoic acids. For example, in an experiment performed at 5 MPa and 230°C, the yields of 2-hydroxy-1-naphthoic, 3-hydroxy-2-naphthoic, and 6-hydroxy-2-naphthoic acids amounted to 14.5, 71.5, and 2.5%.

Surprisingly, the mechanism of the formation of hydroxy naphthoic acids has not been theoretically examined. This work is a DFT study on the mechanism of the carboxylation reaction of **1** in the positions 1 and 3. Since the yield of 6-hydroxy-2-naphthoic acid is very low, the mechanism of its formation is not here considered.

Results and discussion

Before we present our results we need to fix the notation used in this work. **2**, **4**, **6**, and **10** represent intermediates; **3**, **5**, **7**, and **9** stand for transition states; whereas **8** and **12** denote sodium 2-hydroxy-1-naphthoate and sodium 3-hydroxy-2-naphthoate.

Our calculations reveal that the carboxylation reaction in the position 1 of **1** (*i.e.*, the formation of **8**) proceeds *via* three intermediates and three transition states. The reaction in the position 3 of **1** (*i.e.*, the formation of **12**) is a result of a rearrangement from C1 to C3, thus it includes four intermediates and four transition states. The scheme of the mechanism and energetic diagram of the reaction are presented in Fig. 2. The values of the total energies, enthalpies, and free energies of all relevant species are given in Table 1. The bond lengths of all intermediates and transition states, as well as the optimized geometries of some participants in the reaction are presented in Table 2. The values of the natural bond orbital charges for all heavy atoms of the reactands and intermediates are presented in Table 3.

Table 1 and Fig. 2 show that both reaction paths for the carboxylation reaction of **1** are exothermic. Using the free energies, the activation energies for all steps of the reaction are calculated. The activation barriers for the formation of **3** and **5** are relatively low: 36.4 and 33.2 kJ/mol. The high activation energies required for the formation of **9**, **7**, and **11** (197.8, 227.3, and 176.0 kJ/mol) are in agreement
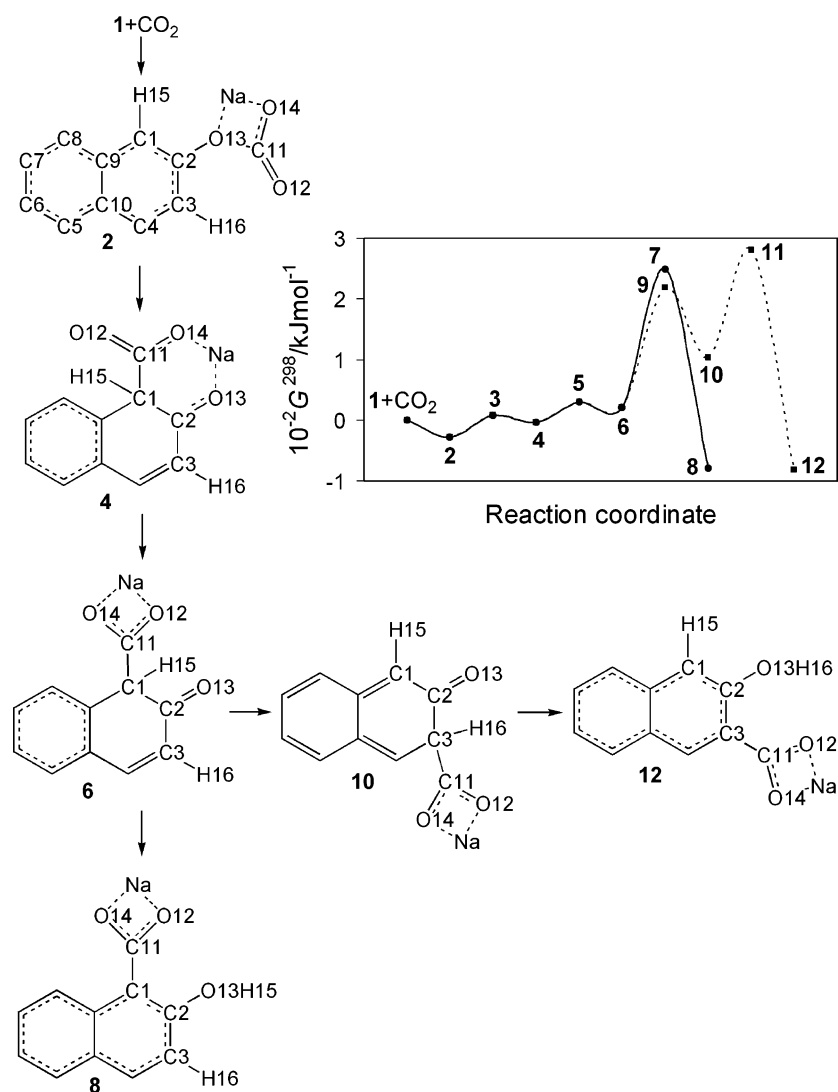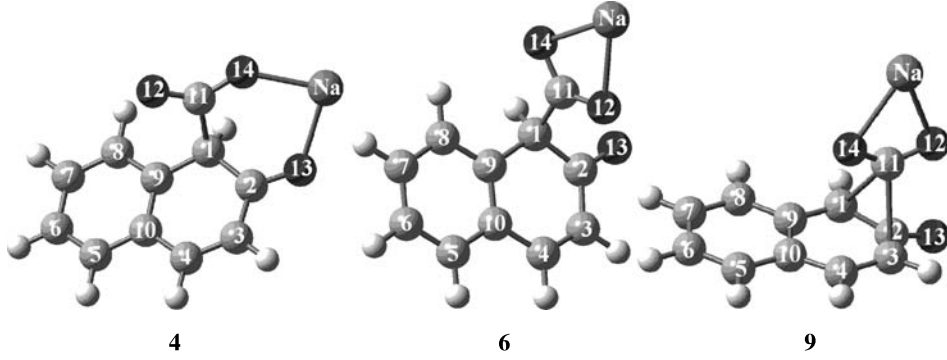
Fig. 2 Mechanism scheme and energy profile for the *Kolbe-Schmitt* reaction of sodium 2-naphthoxide. $1 + CO_2$ – reactands; **2, 4, 6, 10** – intermediates; **3, 5, 7, 9, 11** – transition states; **8, 12** – products. Formation of **8** ●, solid line; formation of **12** ■, dashed line

Table 1 Total energies (E), enthalpies (H^{298}) and free energies (G^{298}) for all participants in the reaction

Species	$-E$/a.u.	$-H^{298}$/a.u.	$-G^{298}$/a.u.
$1 + CO_2$	649.078652	649.064597	649.135542
2	649.105651	649.092159	649.14618
3	649.091469	649.077872	649.13231
4	649.096977	649.083671	649.136807
5	649.085202	649.072683	649.124159
6	649.086775	649.073358	649.12745
7	649.001612	648.988591	649.040872
8	649.127044	649.114431	649.165483
9	649.012274	648.99876	649.05211
10	649.054736	649.041185	649.095927
11	648.989343	648.976231	649.028886
12	649.127875	649.115132	649.166523

with the experimental conditions for the *Kolbe-Schmitt* reaction [5, 7, 8]. They are also in accord with the values for the activation barriers of similar rearrangements, which can be found in Ref. [9–13, 18].

Our calculations reveal that the reaction of **1** with CO_2 begins with the formation of the intermediate sodium 2-naphthoxide-carbon dioxide complex **2**. The natural bond orbital charge distribution of **1** shows (Table 3) that the oxygen and carbons of the naphthalene ring (except the C2 atom) are negatively charged, whereas the positive charge is distributed between the metal and C2. As expected, the carbon of CO_2 is positively charged, whereas the negative charge is distributed between the oxygens. In Fig. 3

Table 2 Optimized geometries for intermediates **4** and **6**, and transition state **9**. Distances between atoms for all intermediates and transition states

| | **4** | | | | **6** | | | **9** | | |
Dist./nm	**2**	**3**	**4**	**5**	**6**	**7**	**9**	**10**	**11**
C1–C2	0.139	0.143	0.150	0.154	0.153	0.147	0.146	0.145	0.140
C2–C3	0.143	0.146	0.146	0.147	0.147	0.142	0.149	0.153	0.148
C3–C4	0.139	0.138	0.137	0.136	0.136	0.138	0.140	0.150	0.143
C4–C10	0.143	0.144	0.145	0.146	0.146	0.145	0.142	0.137	0.141
C5–C10	0.143	0.142	0.142	0.142	0.141	0.142	0.143	0.146	0.144
C5–C6	0.139	0.139	0.140	0.140	0.140	0.139	0.139	0.137	0.138
C6–C7	0.143	0.142	0.141	0.141	0.141	0.142	0.143	0.146	0.144
C7–C8	0.139	0.139	0.140	0.141	0.141	0.140	0.138	0.137	0.138
C8–C9	0.143	0.143	0.141	0.141	0.141	0.142	0.144	0.146	0.144
C9–C10	0.144	0.144	0.142	0.142	0.142	0.144	0.145	0.148	0.147
C1–C9	0.143	0.144	0.150	0.152	0.153	0.147	0.142	0.138	0.142
C1–C11	0.378	0.260	0.170	0.154	0.155	0.153	0.252	0.364	0.371
C3–C11	0.321	0.393	0.360	0.377	0.358	0.367	0.228	0.156	0.155
C2–O13	0.140	0.132	0.129	0.126	0.126	0.132	0.126	0.126	0.134
C11–O12	0.123	0.120	0.125	0.130	0.130	0.130	0.126	0.129	0.129
C11–O14	0.127	0.122	0.129	0.129	0.130	0.130	0.126	0.130	0.130
C11–O13	0.167	0.346	0.313	0.278	0.304	0.299	0.319	0.305	0.304
O12–Na	0.397	0.449	0.435	0.226	0.225	0.224	0.231	0.226	0.226
O13–Na	0.220	0.209	0.220	0.368	0.496	0.507	0.537	0.492	0.516
O14–Na	0.221	0.225	0.212	0.227	0.226	0.225	0.233	0.227	0.227

Table 3 Natural bond orbital charges on heavy atoms in reactands and intermediates. In reactands, atoms C1–Na belong to **1**, whereas C11–O14 belong to CO_2

Atom	$1 + CO_2$	**2**	**4**	**6**	**10**
C1	−0.308	−0.253	−0.442	−0.341	−0.258
C2	0.394	0.342	0.543	0.161	0.530
C3	−0.270	−0.240	−0.291	−0.341	−0.435
C4	−0.201	−0.184	−0.116	−0.297	−0.084
C5	−0.197	−0.191	−0.181	−0.407	−0.172
C6	−0.246	−0.222	−0.217	−0.232	−0.227
C7	−0.222	−0.213	−0.183	−0.231	−0.190
C8	−0.214	−0.202	−0.189	−0.370	−0.200
C9	−0.044	−0.045	0.016	0.303	−0.018
C10	−0.083	−0.064	−0.087	0.313	−0.096
O13	−1.005	−0.814	−0.758	−0.257	−0.604
Na	0.945	0.957	0.955	0.772	0.936
C11	1.016	1.027	0.863	0.273	0.836
O12	−0.508	−0.623	−0.650	−0.496	−0.830
O14	−0.508	−0.799	−0.859	−0.519	−0.809

the HOMOs and LUMOs of **1** and CO_2 are depicted. The LUMO of **1** is located on the metal, whereas the HOMO of CO_2 is located on both oxygens. The HOMO of **1** is delocalized over the naphthlene ring and oxygen. The LUMO of CO_2 is delocalized over all atoms, but the greatest contribution to the LUMO comes from the carbon atom.

Both HOMO–LUMO and charge distribution analyses clearly indicate that the oxygen of CO_2 will bond to the sodium, and the carbon of CO_2 will bind to the adjacent oxygen of **1**, thus forming **2**. This step of the reaction proceeds smoothly, with the stabilization of the system, and without any activation barrier. This is in agreement with the finding that not all chemical reactions proceed *via* transition states, particularly in the gas phase [9–14, 19]. An interesting feature of **2** is that the sodium, carbon, and two oxygen atoms form a four-
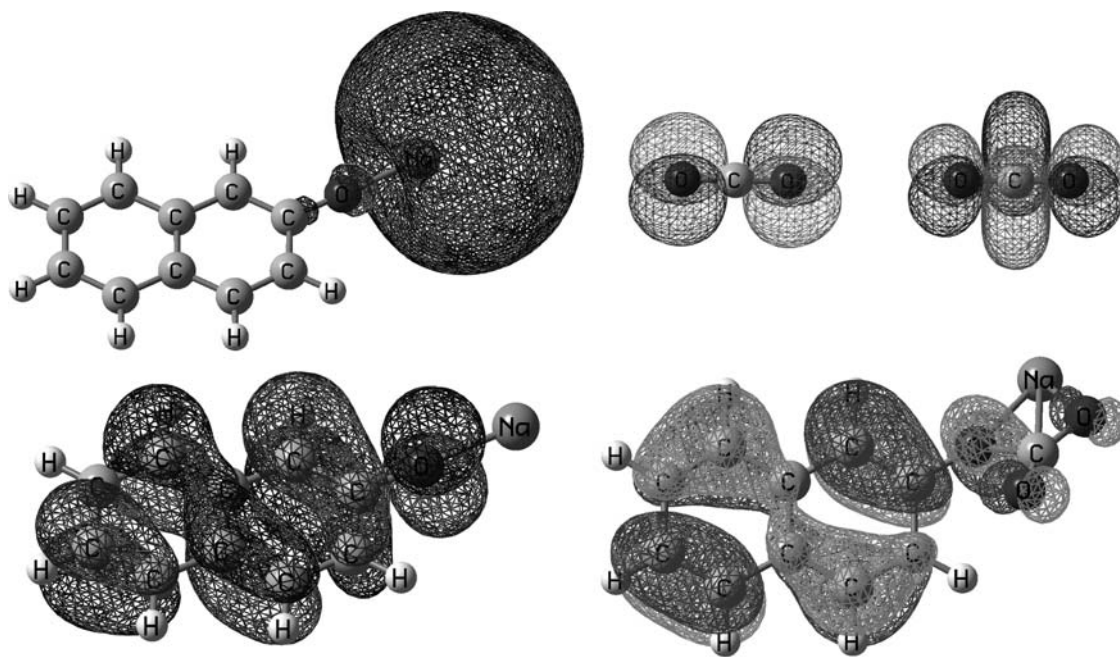
Fig. 3 From left to right: top – LUMO of **1**, HOMO and LUMO of CO₂; bottom – HOMO of **1**, HOMO of **2**

membered ring, where sodium is chelated with O13 and O14 (Fig. 2).

In **2**, the carbon of the CO_2 moiety (C11) is strongly electrophilic, whereas the carbons of the naphthalene ring (except C2) are partially negatively charged (Table 3). The strongest partial negative charge is located on the C1 and C3 atoms. In addition, C1 and C3 are close to the electrophilic C11 (Table 2). On the other hand, the greatest contribution to the HOMO of **2** comes from the C1, C4, C5, C6, and C8 atoms (Fig. 3). Taking into account these facts one can suppose that C11 will perform an electrophilic attack on C1. Our calculations reveal that the reaction in the position 1 proceeds *via* the transition state **3** with the formation of the intermediate **4** (Fig. 2 and Tables 1, 2). An electrophilic attack of C11 on C3 is also examined, but a reaction path in the position 3 is not revealed. Our attempts to optimize a structure analogous to **4**, where C11 is bonded to C3, are not successful either. Although **3** is found at the relatively long C1–C11 distance (Table 2), the transition state is confirmed with the existence of a sole imaginary frequency and the IRC calculations. The results obtained from the IRC calculations for the formation of **3** are presented in Fig. 4. The natural bond orbital analysis of **4** reveals a weak single C1–C11 bond, with 86.0% covalent and 14.0% ionic character. A noticeable ionic character of the C1–C11 bond is in agreement with its length of 0.1705 nm.
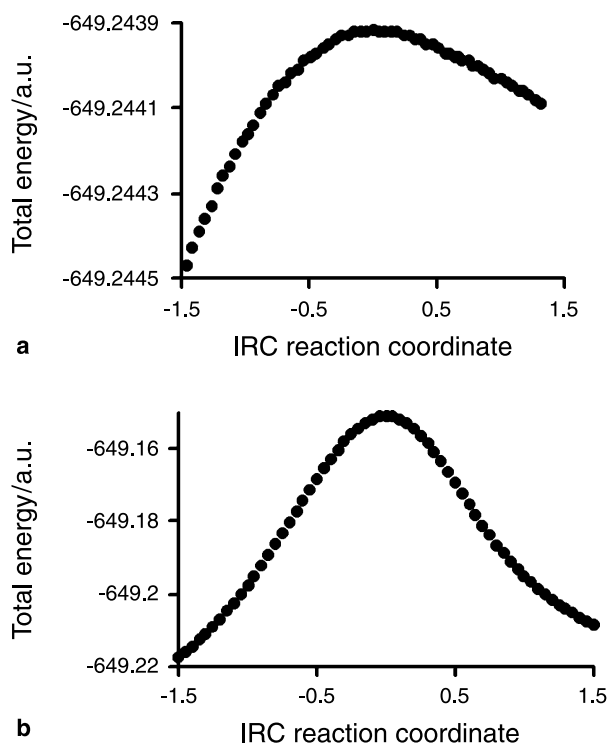

Fig. 4 Plot of total energy versus IRC reaction coordinate for the formation of: a) **3**, b) **7**

The C11–O12 bond of **4** is double, with 16.5% ionic character. The negatively charged O12 is attracted by the positively charged sodium (Table 3). This attraction leads to the formation of the interme-

diate **6** *via* the transition state **5** (Fig. 2 and Table 2). In **5** the C11–O12 bond is single with 33.4% ionic character, whereas in **6** this bond has 33.6% ionic character. The reduction of the order and covalent character of the C11–O12 bond is in accord with a shortening of the O12–Na distance (Table 2). This implies that in **5** and **6** sodium is chelated with the O12 and O14 atoms. The third oxygen atom, O13, is not involved in the chelation, probably due to the short ionic radius of sodium, which does not allow formation of structures where sodium is chelated with **3** oxygens [13].

Figure 2 shows that **6** can undergo two types of transformation. In the first pathway C11 performs an electrophilic attack on C3 (Table 3), whereas in the second pathway O13 performs a nucleophilic attack on H15, whose natural bond orbital charge is 0.257.

The 1,3-shift of hydrogen from C1 to O13 leads to the formation of the product **8**, *via* the transition state **7**. The results obtained from the IRC calculations for the formation of **7** are presented in Fig. 4. In **7** the C1, H15, and O13 atoms form a 3-center hyperbond, where the C1–H15 and O13–H15 distances amount to 0.1489 and 0.1366 nm. The natural bond orbital analysis of **7** confirms the formation of the 3-center hyperbond, with the contributions of the C1–H15 and O13–H15 bonds of 61.5 and 38.5%.

The rearrangement of the CO_2Na group from C1 to C3 leads to the formation of the intermediate **10** *via* the transition state **9** (Fig. 2, Tables 1, 2). An interesting feature of **9** is that C1, C11, and C3 form a bridge over the naphthalene ring. The natural bond orbital analysis of **10** shows that the C1–C11 bond is completely broken, whereas a single C3–C11 bond is formed, with 92.4% covalent character.

Further transformation of **10** is similar to that of **6** in position 1: H16 (whose natural bond orbital charge amounts to 0.290) rearranges from C3 to O13 *via* the transition state **11** (Fig. 2, Table 1). This rearrangement yields the product **12**. In **11** the C3–H16 and O13–H16 distances amount to 0.1393 and 0.1452 nm. Here, a 3-center hyperbond is not observed.

The formation of **9** is more favorable than that of **7** by 29.5 kJ/mol (Table 1). If only this difference in the activation energy is taken into account, it may be concluded that the only product of the carboxylation reaction of **1** will be **12**. But, the formation of **12** requires another high energy barrier, that is the formation of **11**, whose G^{298} is by 61.0 kJ/mol higher

than G^{298} of **9**. On the basis of these facts it can be concluded that at high temperatures both products will be present in the reaction mixture. This is in good accord with the experimental results on the carboxylation reaction of **1** which show that **8** and **12** are major products of the reaction [5, 7, 8]. In addition, the high activation energies required for the formation of **8** and **12** are in agreement with the fact that the reaction mixture needs to be heated above 200°C.

Methods

Geometrical parameters of all stationary points and transition states for the reaction of **1** with CO_2 are optimized in vacuum, employing analytic energy gradients by means of the *Becke*-type three-parameter hybrid combined with the gradient-corrected correlation functional of *Lee et al.* [20, 21]. This functional, commonly known as *B3LYP* [21, 22], implemented in GAUSSIAN98 program package [23], turned out to be quite reliable for geometrical optimizations [24]. The calculations are carried out by employing the LANL2DZ basis set. This basis set proved to be reliable and reproducible for the investigations of the *Kolbe-Schmitt* reaction mechanism [9, 10, 13, 14]. All the fully optimized transition state structures are confirmed by the existence of a sole imaginary frequency, whereas the optimized intermediate structures possess only real frequencies. From the transition state structures, the intrinsic reaction coordinates (IRCs) are obtained, and the free energies are maximized along these paths. The vibrational analysis and the natural bond orbital analysis [25, 26] are performed for all structures. The analysis of the vibrational frequencies is performed by means of the *Molden* program, version 3.7 [27].

Acknowledgements

References

1. Kolbe H (1860) Liebigs Ann 113:125
2. Schmitt R (1885) J Prakt Chem 31:397
3. Daives IA (1928) Z Phys Chem 134:57
4. Hales JL, Jones JI, Lindsey AS (1954) J Chem Soc:3145
5. Lindsey AS, Jeskey H (1957) Chem Rev 57:583
6. Ayres DC (1966) Carbanions in Synthesis. Oldbourne Press, London, p 168
7. Rahim MA, Matsui Y, Kosugi Y (2002) Bull Chem Soc Jpn 75:619
8. Kosugi Y, Imaoka Y, Gotoh F, Rahim MA, Matsui Y, Sakanishi K (2003) Org Biomol Chem 1:817
9. Marković Z, Engelbrecht JP, Marković S (2002) Z Naturforsch 57a:812

10. Marković Z, Marković S, Begović N (2006) J Chem Inf Model 46:1957
11. Stanescu I, Gupta RR, Achenie LEK (2006) Mol Sim 32:279
12. Stanescu I, Achenie LEK (2006) Chem Eng Sci 61: 6199
13. Marković S, Marković Z, Begović N, Manojlović N (2007) Russ J Phys Chem 81:1392
14. Marković Z, Marković S, Manojlović N, Predojević-Simović J (2007) J Chem Inf Model 47:1520
15. Silin NF, Moschtschinkaja NK (1938) J Gen Chem USSR 8:810
16. Gershzon GI (1944) Chem Abstracts 38:1219
17. Chelintsev GV, Smorgonskiĭ LM (1947) Chem Abstracts 41:5466
18. Suenobu K, Nagaoka M, Yamabe T (1999) J Mol Struct (Theochem) 461–462:581
19. Hehre WJ, Shusterman AJ, Huang WW (1996) Laboratory Book of Computational Organic Chemistry, Wavefunction Inc., Irvine
20. Becke AD (1988) Phys Rev A 38:3098
21. Lee C, Yang W, Parr RG (1988) Phys Rev B 37:785
22. Becke AD (1993) J Chem Phys 98:5648
23. Frisch MJ, Trucks GW, Schlegel HB, Scuseria GE, Robb MA, Cheeseman JR, Zakrzewski VG, Montgomery JA Jr, Stratmann RE, Burant JC, Dapprich S, Millam JM, Daniels AD, Kudin KN, Strain MC, Farkas O, Tomasi J, Barone V, Cossi M, Cammi R, Mennucci B, Pomelli C, Adamo C, Clifford S, Ochterski J, Petersson GA, Ayala PY, Cui Q, Morokuma K, Malick AD, Rabuck KD, Raghavachari K, Foresman JB, Cioslowski J, Ortiz JV, Baboul AG, Stefanov BB, Liu G, Liashenko A, Piskorz P, Komaromi I, Gomperts R, Martin RL, Fox DJ, Keith T, Al-Laham MA, Peng CY, Nanayakkara A, Challacombe M, Gill PMW, Johnson B, Chen W, Wong MW, Andres JL, Gonzalez C, Head-Gordon M, Replogle ES, Pople JA (1998) Gaussian 98, Revision A9, Gaussian Inc., Pittsburgh
24. McCoy JD, Nath SK (1996) In: Laird BB, Ross RB, Zeigler T (eds) Chemical Applications of Density Functional Theory. Am Chem Soc, Washington, p 246
25. Foster JP, Weinhold F (1980) J Am Chem Soc 102:7211
26. Reed AE, Weinstock RB, Weinhold F (1985) J Chem Phys 83:735
27. Schaftenaar G (1988) MOLDEN 3.7, CAOS/CAMM Center Netherland